Protein Science (1996), 5:2416–2428. Cambridge University Press. Printed in the USA.

Activator anion binding site in pyridoxal phosphorylase *b*: The binding of phosphite, phosphate, and fluorophosphate in the crystal

NIKOS G. OIKONOMAKOS,[1] SPYROS E. ZOGRAPHOS,[1] KATERINA E. TSITSANOU,[2] LOUISE N. JOHNSON,[2] AND K. RAVI ACHARYA[3]

[1] Institute of Biological Research and Biotechnology, The National Hellenic Research Foundation, 48 Vas. Constantinou Avenue, Athens 11635, Greece
[2] Laboratory of Molecular Biophysics, University of Oxford, Oxford OX1 3QU, United Kingdom
[3] School of Biology and Biochemistry, University of Bath, Claverton Down, Bath BA2 7AY, United Kingdom

(RECEIVED July 31, 1996; ACCEPTED September 25, 1996)

Abstract

It has been established that phosphate analogues can activate glycogen phosphorylase reconstituted with pyridoxal in place of the natural cofactor pyridoxal 5′-phosphate (Chang YC, McCalmont T, Graves DJ. 1983. *Biochemistry* 22:4987–4993). Pyridoxal phosphorylase *b* has been studied by kinetic, ultracentrifugation, and X-ray crystallographic experiments. In solution, the catalytically active species of pyridoxal phosphorylase *b* adopts a conformation that is more R-state–like than that of native phosphorylase *b*, but an inactive dimeric species of the enzyme can be stabilized by activator phosphite in combination with the T-state inhibitor glucose. Co-crystals of pyridoxal phosphorylase *b* complexed with either phosphite, phosphate, or fluorophosphate, the inhibitor glucose, and the weak activator IMP were grown in space group $P4_32_12$, with native-like unit cell dimensions, and the structures of the complexes have been refined to give crystallographic *R* factors of 18.5–19.2%, for data between 8 and 2.4 Å resolution. The anions bind tightly at the catalytic site in a similar but not identical position to that occupied by the cofactor 5′-phosphate group in the native enzyme (phosphorus to phosphorus atoms distance = 1.2 Å). The structural results show that the structures of the pyridoxal phosphorylase *b*-anion-glucose-IMP complexes are overall similar to the glucose complex of native T-state phosphorylase *b*. Structural comparisons suggest that the bound anions, in the position observed in the crystal, might have a structural role for effective catalysis.

Keywords: binding, fluorophosphate, phosphate, phosphite, pyridoxal phosphorylase, T state

Glycogen phosphorylase (GP) catalyzes the first step in the intracellular degradation of glycogen into glucose 1-phosphate (Glc-1-*P*). It is controlled by shifts in an equilibrium between several conformational states, depending on the phosphorylation state and the binding of various allosteric effectors, and ranging from a low affinity T state to a high affinity R state (in the nomenclature of Monod et al., 1965). In resting muscle the enzyme exists in the inactive form (GP*b*), which can be activated either by covalent phosphorylation to form GP*a* or by noncovalent cooperative binding of AMP, IMP, or analogues (Graves & Wang, 1972; Madsen, 1986; Johnson et al., 1989). Its nucleotide-dependent activity is inhibited by Glc-6-*P*, ATP, and other metabolites, such as glucose (Glc), which maintain the enzyme in an inactive state and are responsible for the fine control of glycogenolysis *in vivo* (Newgard et al., 1989). GP*a*, even at relatively low concentrations, and GP*b*, at fairly high concentrations, when activated, associate to form tetramers. Binding to glycogen dissociates the tetrameric form to dimers. Consequently, the catalytically active molecular species of GP is the dimer. Tetramers still retain some activity, but may be dissociated by T-state effectors such as Glc to give fully inactive dimers (Oikonomakos et al., 1992, and references therein).

Crystal structures of the four basic conformational states of the muscle enzyme—T-state GP*b* (Acharya et al., 1991)—T-state GP*a* (Sprang et al., 1988), R-state GP*b* (Barford & Johnson, 1989; Sprang et al., 1991), and R-state GP*a* (Barford et al., 1991)—are

Reprint requests to: Nikos G. Oikonomakos, The National Hellenic Research Foundation, Institute of Biological Research and Biotechnology, 48 Vas. Constantinou Avenue, Athens 11635, Greece; e-mail: nikos@apollon.servicenet.ariadne-t.gr.

Abbreviations: GP, glycogen phosphorylase, 1,4-α-glucan:orthophosphate α-glucosyltransferase (EC 2.4.1.1); GP*b*, glycogen phosphorylase *b*; GP*a*, glycogen phosphorylase *a*; PLP, pyridoxal 5′-phosphate; PL, pyridoxal; DPL, 5′-deoxypyridoxal; PLPMe, pyridoxal 5′-phosphate monomethyl ester; PLDP, pyridoxal 5′-diphosphate; Glc, α-D-glucose; 1-GlcNAc, 1-acetyl-β-D-glucopyranosylamine; NJT, nojirimycin tetrazole; Glc-1-*P*, α-D-glucose 1-phosphate; heptenitol, 2,6-anhydro-1-deoxy-D-*gluco*-hept-1-enitol; heptulose-2-*P*, 1-deoxy-D-*gluco*-heptulose 2-phosphate; Bes, N,N-bis(2-hydroxy-ethyl)-2-aminomethane sulphonic acid; DTT, dithiothreitol.

available, and these have provided the molecular basis for understanding the allosteric and catalytic properties of the enzyme. On conversion from the T to R state there are substantial changes in quaternary structure that are correlated with changes in tertiary structure. The greatest changes in tertiary structure take place at the subunit–subunit contacts and these result indirectly in shifts of residues at the catalytic site. The 280s loop (residues 282–286), which blocks access from the bulk solvent to the catalytic site, is disordered and is displaced from the catalytic site. Arg 569 occupies the position close to that occupied by Asp 283 in the T state, and the interchange between an acidic and a basic group helps to create the substrate phosphate recognition site. These shifts not only create a high affinity phosphate site but also promote a favorable electrostatic environment for the 5′-phosphate group of the essential cofactor pyridoxal 5′-phosphate (PLP) (Johnson, 1992).

GP is completely dependent on the coenzyme PLP for activity and the role of 5′-phosphate group in catalysis has been shown to be quite different from the conventional vitamin B_6 dependent enzymes (Fischer et al., 1958). Removal of the cofactor results in inactivation, but the apoenzyme can be fully reactivated by reconstitution with PLP. Reconstitution experiments with a number of modified cofactors (Madsen & Withers, 1986; Johnson et al., 1989; Palm et al., 1990) have demonstrated that the 5′-phosphate plays an obligatory role in catalysis. Only PLP analogues with a dianion that can be protonated such as $-OPO_3^{2-}$ or $-CH_2PO_3^{2-}$ in position 5 give significant activity. The enzyme reconstituted with pyridoxal (PL) is inactive, but addition of dianions such as phosphite, fluorophosphate, phosphate, and some analogues can confer activity, indicating that these anions may bind at the subsite occupied by the coenzyme 5′-phosphate in the native GP (Parrish et al., 1977; Chang et al., 1983). The observation that phosphite activation of PL-GP can be reversed by pyrophosphate, a potent inhibitor of the enzyme, strictly competitive with both anion and Glc-1-*P* (Parrish et al., 1977; Chang et al., 1983), implied the adjacent positions of activator anion and substrate phosphate in the catalytic site. ^{31}P-NMR studies have shown that the 5′-phosphate group of PLP is a monoanion in the T-state conformation and a dianion in the R-state conformation. When the substrates or inhibitors bind, there is a change in the ^{31}P chemical shift, which has been interpreted either as a partially protonated monoanionic form or as a tightly coordinated and distorted dianion (Feldman & Hull, 1977; Withers et al., 1981). These studies combined with kinetic and crystallographic evidence led to two main proposals for the role of the coenzyme 5′-phosphate in the catalytic mechanism: i.e., that it functions (1) as a proton donor-acceptor shuttle in general acid-base catalysis (Johnson et al., 1989; Palm et al., 1990) or (2) as an electrophilic "constrained" dianion (Madsen & Withers, 1986). Both proposals require the coenzyme 5′-phosphate and the substrate phosphate to be directly interacting. The interacting phosphates hypothesis was confirmed crystallographically in the analysis of the transition-state intermediate-like GP*b*-heptulose 2-*P* complex (McLaughlin et al., 1984; Hajdu et al., 1987; Johnson et al., 1990), which showed a close *P*-*P* distance (of phosphorus atoms of phosphate to cofactor 5′-phosphate) of 4.8 Å. These studies and recent structural studies on the T- and R-state GP*b*-NJT-phosphate complexes (Mitchell et al., 1996) have definitively established the location of the substrate phosphate at or near the transition state of the reaction and are consistent with the proposed role for the cofactor 5′-phosphate as a general acid.

A main criticism against proton donor-acceptor function for the 5′-phosphate of the cofactor has been based on the finding that fluorophosphate (pK_a = 4.8), which induces activity in PL-GP (13% of the activity of the native PLP-GP*b*), cannot become protonated at pH 6.8 where the enzyme is active (Parrish et al., 1977). The pH dependencies of the PL-GP using phosphite (pK_a = 6.6) or fluorophosphate as activator anions are also unaltered, despite the difference in the pK_a values of these anions (Withers et al., 1982c). Furthermore, ^{19}F-NMR spectra of the bound fluorophosphate activator also showed that no change in its ionization state occurred on binding or during catalysis (Chang et al., 1983), a result not in accord with a role for the cofactor 5′-phosphate as a proton donor in catalysis. Based on these results and other results from kinetic and ^{19}F-NMR experiments of GP*b* reconstituted with 6-fluorinated PL and DPL, Chang et al. (1987) suggested that the cofactor 5′-phosphate is mainly a structural determinant holding other groups in the correct orientation for catalysis. PL-GP*b* provides a good enzyme derivative to study possible functions of the cofactor 5′-phosphate in GP catalysis (Chang et al., 1983, 1987). On the basis of tertiary and quaternary structural information deduced from ^{31}P-NMR and ultracentrifugation data (Withers et al., 1982b), it has been shown that PL-GP*b* is an allosteric enzyme whose R state can quite easily be pushed into a T-state conformation by phosphite and Glc. Previous characterization of the T-state PL-GP*b*-phosphite-Glc-IMP complex structure at 2.4 Å resolution (Oikonomakos et al., 1987) has led to the assignment of the phosphite position that is close to but distinguishable from the position of the coenzyme 5′-phosphate. In this study, detailed kinetic and sedimentation velocity experiments have characterized the R- and T-state conformations of PL reconstituted GP*b*. X-ray studies on the co-crystallized PL-GP*b*-phosphite-Glc-IMP, PL-GP*b*-phosphate-Glc-IMP and PL-GP*b*-fluorophosphate-Glc-IMP complexes are described in order to further investigate the mode of anion binding to the modified enzyme in the crystal. The refined 2.4 Å resolution structures show that the anions bind in an identical position to the catalytic site and provide significant stability to the crystal structure of PL-GP*b* (T state) through a number of polar contacts. The structural results also provide an explanation for the solution properties of the enzyme and rationalize previous kinetic observations with DPL-GP*b*.

Results

Kinetics

The kinetic properties of phosphite activated PL-GP*b* (as compared with those of the native GP*b*) are summarized in Table 1. Initial rates were measured in the presence of varying concentrations of phosphite and Glc-1-*P* at constant saturating concentrations of AMP (1 mM) and glycogen (1%) and data analyzed by double-reciprocal plots (data not shown). Straight lines were obtained approximately converging at the *x* axis, in agreement with the proposed bi-reactant sequential mechanism (Chang et al., 1983). The equation based on this kinetic model (Scheme I), similar to one described previously by Segel (1975) was added to GraFit (Leatherbarrow, 1992) using the built-in equation editor. The program then determines all the dissociation constants and V_{max} simultaneously by fitting all of the data at once. The values were similar to those reported previously (Parrish et al., 1977; Chang et al., 1983, 1987) except for those for Glc-1-*P*. The K_s and αK_s values were reported to be 18 and 22 mM, respectively (Chang et al., 1983). The discrepancy might be due to different enzyme preparations. PL-GP*b*, compared with native GP*b*, shows a reduc-

Table 1. *Kinetic parameters of native GPb and PL reconstituted GPb*

Additions	Parameters
Native GP*b* vs Glc-1-*P*	V_{max} = 71.7 ± 2.2 IU[a]
	K_m = 2.5 ± 0.2 mM[a]
Native GP*b* vs Glc-1-*P* + Glc	K_i = 3.4 ± 0.1 mM
	(n = 1.5 ± 0.1)[b]
Native GP*b* vs AMP	V_{max} = 71.6 ± 3.0 IU[c]
	K_m = 37 ± 9 μM
	(n = 1.5 ± 0.1)[c]
Native GP*b* vs IMP	V_{max} = 20.1 ± 0.2 IU[d]
	K_m = 1.2 ± 0.1 mM
	(n = 1.5 ± 0.1)[d]
PL-GP*b* vs Glc-1-*P* or phosphite	V_{max} = 10.8 ± 0.2 IU[e]
	K_s = 11.2 ± 2.5 mM[e]
	αK_s = 10.0 ± 3.4 mM[e]
	K_a = 0.63 ± 0.12 mM[e]
	αK_a = 0.55 ± 0.18 mM[e]
PL-GP*b* vs AMP	V_{max} = 7.6 ± 0.3 IU[f]
	K_m = 22 ± 7 μM
	(n = 1.6 ± 0.1)[f]
PL-GP*b* vs IMP	V_{max} = 3.5 ± 0.1 IU[g]
	K_m = 1.4 ± 0.1 mM
	(n = 1.5 ± 0.1)[g]
PL-GP*b* vs phosphite + Glc	K_i = 73 ± 5 mM[h]
PL-GP*b* vs Glc-1-*P* + Glc	K_i = 142 ± 2 mM
	(n = 1.6 ± 0.1)[i]
PL-GP*b* vs Glc-1-*P* + Glc	K_i = 75 ± 1 mM
	(n = 1.8 ± 0.1)[j]

Enzymes' activities were determined as described in Materials and methods at 30 °C and pH 6.8 in a buffer consisting of 20 mM β-glycerophosphate, 15 mM 2-mercaptoethanol, 0.5 mM EDTA at a constant concentration of glycogen (1%).

[a] Measured in the presence of 1 mM AMP and varied concentrations of Glc-1-*P* (3–40 mM) from double-reciprocal plots. IU is in μmol/mg/min.

[b] Measured at a constant concentration of AMP (1 mM) and various concentrations of Glc-1-*P* (3–40 mM) and Glc (5, 10, and 15 mM). Kinetic data were transformed into Hill plots for Glc-1-*P*, which yielded the apparent K_m values and Hill coefficient n (given in parenthesis). K_i was calculated from the secondary plot of the apparent K_m values versus inhibitor concentration.

[c] Measured at a constant concentration of Glc-1-*P* (40 mM) and various concentrations of AMP (0.015–1 mM) by a means of a Hill plot for AMP.

[d] As in footnote c except that AMP was replaced by IMP at concentrations of 0.5, 1, 2, 3, and 4 mM.

[e] Measured at a constant concentration of AMP (1 mM) and various concentrations of Glc-1-*P* (5–40 mM) and phosphite (0.5–6.0 mM). Best fit lines were computer generated according to the random mechanism based equation (see Scheme I).

[f] Measured at constant concentrations of Glc-1-*P* (40 mM) and phosphite (6.0 mM) and various concentrations of AMP (0.005–1 mM) by means of a Hill plot for AMP.

[g] Measured at constant concentrations of Glc-1-*P* (40 mM) and phosphite (6.0 mM) and various concentrations of IMP (0.5–6.0 mM) by means of a Hill plot for IMP.

[h] Measured at constant concentrations of AMP (1 mM) and Glc-1-*P* (40 mM) and various concentrations of phosphite (0.5–6.0 mM) and Glc (100, 200, and 300 mM) by means of computer generated best fit lines according to the equation for uncompetitive inhibition (see Scheme I).

[i] Measured at constant concentrations of AMP (1 mM) and phosphite (0.5 mM) and various concentrations of Glc-1-*P* (5–40 mM) and Glc (100, 200, and 300 mM) as in footnote b.

[j] As in footnote i except that the concentration of phosphite was 6.0 mM.

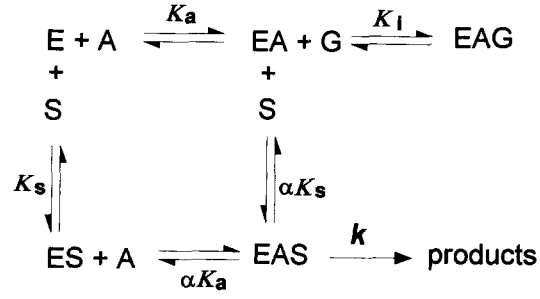

Scheme I. Kinetic scheme for the inhibition of phosphite activated PL-GP*b* by Glc. E, A, S and G represent the enzyme-glycogen-AMP complex, phosphite, Glc-1-*P*, and Glc, respectively. The rate equation for this scheme is $V_{max}/v = 1 + \alpha K_s/[S] + \alpha K_s[G]/K_i[S] + \alpha K_a(1 + K_s/[S])/[A]$, where K_a and αK_a are respectively the dissociation constants of phosphite from enzyme-AMP-glycogen and enzyme-AMP-glycogen-Glc-1-*P* complexes; K_s and αK_s, the dissociation constants of Glc-1-*P* from enzyme-AMP-glycogen and enzyme-AMP-glycogen-phosphite complexes; and K_i, the dissociation constant of Glc from the enzyme-AMP-glycogen-phosphite complex.

tion in V_{max} (10.8 μmol/mg/min) and a four-fold increase in K_m (10.0 mM) with respect to Glc-1-*P*. The extent of PL-GP*b* activation by AMP and IMP was examined. PL-GP*b* shows a K_m value of 22.1 μM and a Hill coefficient (n) value of 1.6 for AMP binding. The K_m value for AMP obtained in this study compares well with the value of 25 μM obtained by Parrish et al. (1977). The K_m value for the weak activator IMP was changed a little (compared with the native enzyme). All of the above results show that PL-GP*b* retains most of the kinetic properties of the native, except for the lower V_{max} values.

The effect of Glc, an effective allosteric inhibitor for the native GP with K_i values in the low mM range (Sprang et al., 1982; Martin et al., 1991), on the kinetic properties of PL-GP*b* with respect to both phosphite and Glc-1-*P* was also studied. An uncompetitive kinetic behavior was observed for Glc in inhibiting PL-GP*b* with respect to phosphite (K_i = 73 mM), but competitive kinetics were found for Glc binding with respect to Glc-1-*P*, in agreement with the kinetic predictions made by Withers et al. (1982a). Furthermore, as the concentration of phosphite was increased from 0.5 mM to 6.0 mM, a two-fold decrease in K_i value for Glc was observed (Table 1). This result may indicate that the presence of phosphite contributes to Glc binding.

Ultracentrifugation

Sedimentation experiments were performed under conditions similar to those employed in the co-crystallization experiments. In the absence of ligands, the enzyme exists as a dimer ($s_{20,w}$ = 8.5 S) but on addition of 2 mM IMP and 2 mM spermine, complete tetramerization occurred ($s_{20,w}$ = 13.1 S). Subsequent addition of either phosphite (1 mM) or Glc (50 mM) had no further effect on its quaternary structure. However, in the presence of 1 mM phosphite, Glc when added in increasing amounts promoted dissociation into a dimeric form $s_{20,w}$ = 8.4 S). β-Glycerophosphate, a commonly used buffer in GP work and an inhibitor of the enzyme at high concentrations, binds to the allosteric site of GP*b* (Oikonomakos et al., 1989) but it does not bind to the catalytic site and thereby cannot skew the equilibrium. Thus, PL-GP*b*, in the presence of IMP, spermine, phosphite, and Glc, represents an associating-dissociating system and this property of the enzyme to change to

different dimer to tetramer ratios in titration with Glc was used to investigate in detail the effect of Glc concentration on the extent of protein dissociation. In control experiments, protein samples with different Glc concentrations and constant concentrations of IMP (2 mM), spermine (2 mM) and phosphite (1 mM) were preincubated in the cells for 30, 60, and 120 minutes at 20 ± 1 °C before centrifugation at 50,000 rpm, but the extents of dissociation did not practically change, indicating that the establishment of the new equilibrium (in the presence of a given Glc concentration) under the employed conditions was immediate. When the percentage of tetramer (y) is plotted as a function of Glc concentration (x) by applying the Hill equation provided by GraFit (Leatherbarrow, 1992),

$$y = \alpha/(1 + (x/K_{0.5})^s),$$

where α is the maximum y range, $K_{0.5}$ is the Glc concentration at which $y = \alpha/2$, and s is a slope factor measured by plotting $\log y/(\alpha - y)$ versus $\log x$, the resulting curve representing the Glc-induced quaternary change of the enzyme is sigmoidal and yields an apparent $K_{0.5}$ value of 7.5 ± 0.2 mM for the Glc effect (Fig. 1). The corresponding value for the dissociation of the complex enzyme-AMP-glycogen-phosphite-Glc, calculated from the kinetic experiments, is 75 mM in the presence of 6.0 mM phosphite (Table 1).

X-ray crystallography

Crystallographic data collection, processing, and refinement statistics for the three co-crystallized PL-GP*b*-anion-Glc-IMP complexes are shown in Table 2. For all complexes, the electron density difference maps (against native T-state GP*b*) (Acharya et al., 1991) showed a negative peak that appeared in the position of the 5′-phosphate of the native enzyme, positive peaks representing the binding of the anion and Glc at the catalytic site, and concomitant changes of the enzyme, normally observed on binding Glc (e.g., Martin et al., 1990) indicating a small movement of His 377 away from the sugar in order to optimize contacts to O-6 of Glc and displacement of a water molecule, Wat 9.904. Other features of the difference maps included shifts of six water molecules, Wat 1.895, Wat 0.879, Wat 0.885, Wat 3.896, Wat 8.896, and Wat 1.897, located at the catalytic site. Additional density at the allosteric site showed strong binding of IMP. There were also indications in the difference maps for shifts in the guanidinium group of Arg 309 such that the nucleotide phosphate at the allosteric site is coordinated to both Arg 309 and Arg 310. The positions of the peaks were exactly the same for all the three complexes. In a previous crystallographic study of the PL-GP*b*-phosphite-Glc-IMP (Oikonomakos et al., 1987), the positions of the phosphite oxygens could not be defined. However, double difference Fourier maps, calculated using as coefficients ($F_{\text{PL-enzyme-phosphate-Glc-IMP}} - F_{\text{PL-enzyme-phosphite-Glc-IMP}}$) and ($F_{\text{PL-enzyme-fluorophosphate-Glc-IMP}} - F_{\text{PL-enzyme-phosphite-Glc-IMP}}$) revealed an extra strong positive peak, suggesting that one of the phosphate oxygen (or the fluorine) might be located there. This enabled us to approximately position the bound anions for subsequent crystallographic refinement. In fact, the X-PLOR refinement of the PL-GP*b*-phosphite-Glc-IMP complex showed that the phosphite anion binds in such a way that its three oxygen atoms are positioned toward O-5 of the PL and not away from the PL as assigned previously (Oikonomakos et al., 1987).

The electron density for the PL molecule and anions as bound to T-state GP*b* are shown in Figure 2. The difference electron density maps for PL-GP*b*-phosphate-Glc-IMP and PL-GP*b*-fluorophosphate-Glc-IMP complexes against PL-GP*b*-phosphite-Glc-IMP complex, in the vicinity of the catalytic site, are shown in Figure 3. In the X-PLOR refined structures of the three complexes, the conformational changes in the enzyme are small and similar to those observed when Glc (Martin et al., 1990) or a Glc-like inhibitor (Martin et al., 1991; Oikonomakos et al., 1995) binds. We describe in some detail mainly the PL-GP*b*-phosphate-*b*-Glc-IMP complex.

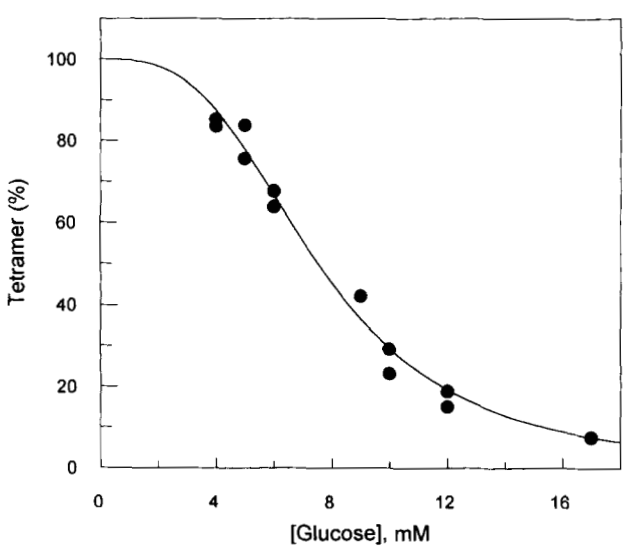

Fig. 1. The effect of Glc on the dissociation of PL-GP*b* in the presence of 2 mM IMP, 2 mM spermine, and 1 mM phosphite. Sedimentation velocity measurements (in duplicate) were performed at a rotor speed of 50,000 rpm and 20 ± 1 °C with 10 mg/ml enzyme in 7 mM β-glycerophosphate (pH 6.8), 7 mM 2-mercaptoethanol buffer as described under Materials and methods.

Interactions between IMP and allosteric site residues

In the crystallization mixture the IMP concentration was 2.0 mM. The electron density suggests that the nucleotide is tightly bound at the allosteric site (data not shown). The fit to the electron density was satisfactory. The model was fitted C-3′-*endo* conformation for the ribose, the orientation of the base was *anti*, and the conformation of the C-4′-C-5′ and C-5′-O-6′ bonds was *gauche* and *trans*, respectively. The position and conformation are similar with those observed for the refined structure of the T-state GP*b*-AMP complex (Barford et al., 1991). However, this conformation differs from the single crystal structure of IMP (Rao & Sundaralingam, 1969; Spiram et al., 1991). The interactions formed between IMP and the allosteric site consist of salt bridges between the side chains of Arg 309 and Arg 310 of α8 helix (residues 289–314) to the phosphate of IMP. The O-2′ of the ribose moiety is hydrogen-bonded to Asp 42′ (3.2 Å) from the symmetry related subunit. No specific interactions are made to the nucleotide base, except that the side chain of Tyr 75 of α2 helix (residues 47–78) is stacked co-parallel with the base at a distance of 3.5 Å. In general, the interactions made are characteristic of the T-state conformation at this site, which differs from the R-state conformation observed in the binding of AMP to GP*a* (Sprang et al., 1988) and GP*b* (Barford et al., 1991; Sprang et al., 1991).

Table 2. *Statistics of data processing and refinement for PL-GPb-anion-α-Glc-IMP complexes*

	HPO_3^{2-}	HPO_4^{2-}	PFO_3^{2-}
No. of reflections measured	98,321	103,280	115,457
No. of unique reflections	32,351	31,054	33,853
Completeness of data	85.9%	81.8%	88.8%
$R_m(I)$	0.074	0.064	0.077
$R_{iso}(F)$	0.122	0.112	0.115
Initial R factor	0.228	0.234	0.215
No. of atoms in final cycle of refinement	8,370	8,371	8,370
No. of water molecules in final cycle	562	562	562
No. of reflections used in refinement (8–2.4 Å, $I > 0$)	31,577	30,143	32,907
Final R factor	0.192	0.185	0.185
RMSD in bond lengts	0.017Å	0.018Å	0.018Å
RMSD in bond angles	3.5 degrees	3.4 degrees	3.4 degrees

Merging R_m is defined as $R_m = \Sigma_i\Sigma_h|\langle I_h\rangle - I_{ih}|/\Sigma_i\Sigma_h I_{ih}$, where $\langle I_h\rangle$ and I_{ih} are the mean and ith measurement of intensity for reflection h, respectively. R_{iso} is the mean fractional isomorphous difference in structure factor amplitudes from native T-state GP*b*. Crystallographic R factor is defined as $R = \Sigma||F_o| - |F_c||/\Sigma|F_o|$, where $|F_o|$ and $|F_c|$ are the observed and calculated structure factor amplitudes, respectively.

Interactions between Glc and catalytic site residues

The mode of binding and the interactions that Glc makes with PL-GP*b* in the presence of phosphate are almost identical with those previously reported for GP*b*-Glc (Martin et al., 1990). In particular, Asp 283 and Asn 284 of the 280s loop are in the same position where they are found in the GP*b*-Glc complex. Also the refined PL-GP*b*-phosphate-Glc-IMP complex structure was essentially identical to the structure of the native GP*b*-Glc complex and showed the same conformational shifts as the Glc complex from the native T-state GP*b* structure (for example, a small shift of His 377 away from the glucopyranose moiety in order to accommodate the O-6 hydroxyl) at the catalytic site.

Interactions between PL and phosphate and catalytic site residues

In the PL-GP*b*-phosphate-Glc-IMP complex, the PL (Scheme II) occupies an almost identical position to its counterpart in native PLP-GP*b* and makes similar polar and van der Waals contacts to the enzyme. The PL ring has altered its position only slightly (0.2–0.3 Å), but the shifts are too small to change the hydrogen bonds or the van der Waals contacts. Water molecules, Wat 2.895, which links O-5 atom of the pyridoxal ring with Tyr 648, was shifted slightly (0.3 Å), and Wat 3.896, which links N-1 atom of PL with a hydrogen bond network involving a second water molecule (Wat 0.884), Tyr 90, and Asn 133, was shifted 0.8 Å from its initial position in the native structure. The phosphate anion binds between PL and Glc and is located close to but separate from the 5′-phosphate binding site of the native enzyme. The phosphorus positions of phosphite, fluorophosphate, and phosphate are identical and all are located 1.2 Å from PLP phosphorus. In the native PLP-GP*b*, the cofactor 5′-phosphate is hydrogen bonded to one basic group (Lys 568), to two main-chain N (Thr 676 and Gly 677) at the start of the α-21 helix (residues 676–686), and to four buried structural waters (Wat 1.895, Wat 0.879, Wat 0.885, and Wat 1.897) that in turn make additional hydrogen bonds to protein atoms (Oikonomakos et al., 1987; Acharya et al., 1991). The present structural results indicate that activator anion can be accommodated at the catalytic site with essentially no disturbance of the structure, and the interactions it makes are similar but not identical to those observed for the 5′-phosphate group of PLP in native enzyme. Thus, as a result of the different position of the anion, as compared with the cofactor 5-phosphate group, the anion is placed closer, within a hydrogen bond distance, to the NZ of Lys 574 (2.6–2.8 Å as compared with 4.5 Å in native structure), while the hydrogen bonds of the 5′-phosphate group to Thr 676 and Gly 677 are no longer existent in the PL-GP*b*-anion-Glc-IMP complexes. In the PL-GP*b*-fluorophosphate-Glc-IMP and PL-GP*b*-phosphate-Glc-IMP complex structures (compared with the native PLP-GP*b* structure) shifts of approximately 0.5–0.7 Å are seen in the positions of the four internal bound waters Wat 0.885, Wat 0.879, Wat 1.895, and Wat 1.897, but these shifts do not appear to affect the rest of the protein structure. The same shifts are also seen in the PL-GP*b*-phosphite-Glc-IMP complex, except that Wat 0.885 is displaced (or binds weakly). In all three complexes the guanidinium group of Arg 569 is in its buried position, as observed in the native T-state GP*b* (Acharya et al., 1991) and its charged group is compensated by hydrogen bonds to the carbonyl oxygens of Asn 133, Pro 281, and Lys 608.

In PL-GP*b*-phosphate-Glc-IMP complex structure, phosphate anion makes a total of 7 hydrogen bonds (Fig. 4, Table 3) and 29 van der Waals interactions, of which 24 are to protein atoms and 5 to PL (not shown). Phosphate oxygen O-1 makes a direct contact to O-5 of PL and is linked to O-4 hydroxyl group of Glc and Thr 676 via a water molecule (Wat 1.897). Phosphate oxygen O-2 makes contact to Wat 0.885, which in turn makes a direct contact to Gln 665 and two indirect contacts with Ser 674 and Gln 696 via a second water molecule (Wat 9.896). Phosphate oxygen (O-3) interacts directly with O-5 of PL, a basic group (Lys 568), and Wat 1.895; the latter is involved in an extensive network of hydrogen bonds (Table 3). Phosphate O-4 makes hydrogen-bonds to the NZ of Lys 574 and Wat 0.879, which in turn interacts with the main-chain NH group of Arg 569. A structural analysis of phosphate and sulphate binding sites in 38 proteins showed that the average number of contacts per phosphate group is 3.5 (±2.3) (Copley & Barton, 1994). This suggests that the phosphate anion, which makes a total of 7 polar contacts with PL-GP*b*, is tightly bound. This is also reflected in a relatively low average *B*-factor for the phosphate anion (23 $Å^2$), compared with an average *B*-factor of 21 $Å^2$ for main-chain atoms in the complex.

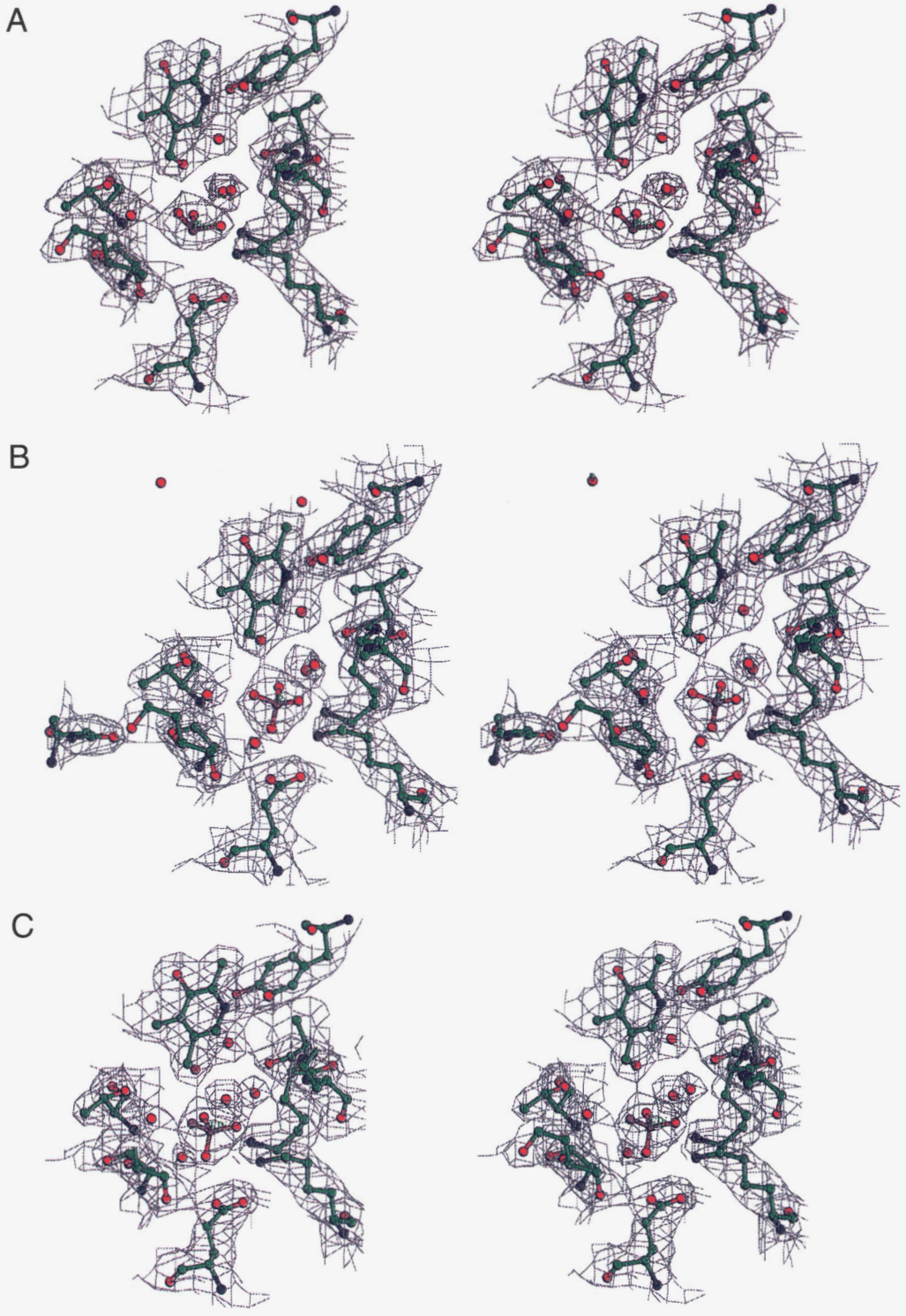

Fig. 2. Stereo diagrams of the catalytic site of the refined PL-GP*b*-phosphite-Glc-IMP (**A**), PL-GP*b*-phosphate-Glc-IMP (**B**) and PL-GP*b*-fluorophosphate-Glc-IMP (**C**) complexes showing bound anions and Glc and electron densities from the $2F_o - F_c$ maps. The contour levels correspond to approximately 1 RMSD of the maps.

Comparison with a transition-state, intermediate-like complex

Nojirimycin tetrazole (NJT) has been shown to be a potent inhibitor of the α-glucosidase from *Agrobacter* with a K_i value of 1.4 μM (Ermert et al., 1993). Since it was proposed that this compound might act as a transition-state analogue for the α-glycosidase catalysis and mimic the trigonal geometry required at C-1 for the formation of the carbonium ion intermediate, its interactions with GP*b* were investigated by kinetic and crystallographic methods (Mitchell et al., 1996). NJT was found to be a competitive inhibitor with respect to Glc-1-*P*, with a K_i value of 0.70 mM, but it binds

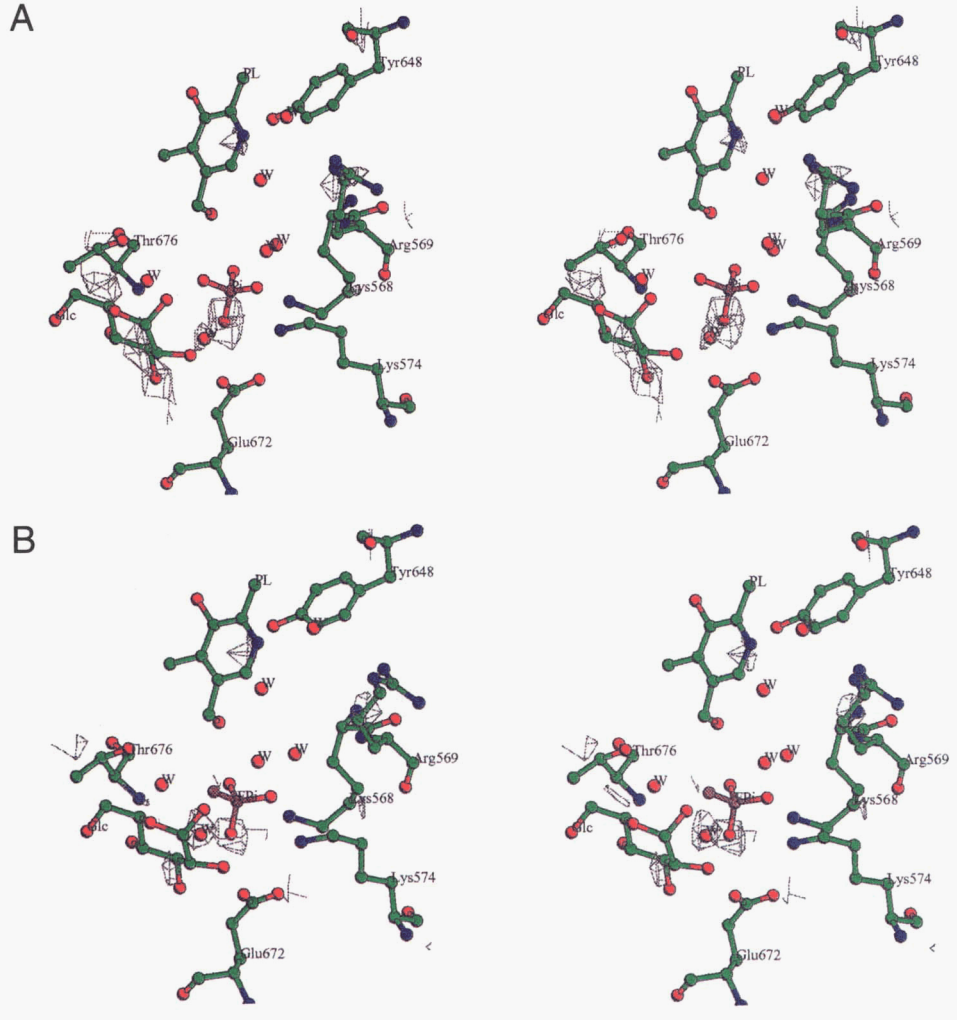

Fig. 3. Difference Fourier syntheses in the vicinity of the catalytic site for PL-GP*b*-phosphate-Glc-IMP (**A**) and PL-GP*b*-fluorophosphate-Glc-IMP (**B**) complexes against PL-GP*b*-phosphite-Glc-IMP complex. The X-PLOR refined coordinates for PL-GP*b*-phosphate-Glc-IMP (**A**) and PL-GP*b*-fluorophosphate-Glc-IMP (**B**) are shown. Single positive contour levels at 700 arbitrary units (approximately three times the standard deviation of the difference electron densities) are shown. PL, Glc and selected amino acids are also shown.

strongly to the enzyme-AMP-glycogen-phosphate complex with a K_i value of 53 μM, a result indicating that the complex enzyme-AMP-glycogen-NJT-phosphate may mimic a structure close to the transition state. A crystallographic binding study by diffusion of the NJT and phosphate into preformed crystals of T-state GP*b* showed that both the NJT molecule and the phosphate ion bind tightly at the catalytic site. The NJT on binding to GP*b* adopts a well defined half-chair conformation; its binding is dominated by contacts from O-2, O-3, O-4, and O-6 to catalytic site residues that are essentially identical to those made by Glc (Martin et al., 1990). The phosphate binds in a site between the cofactor 5′-phosphate and NJT in a position very close to the postulated attacking site (Hajdu et al., 1987; Duke et al., 1994) and the refined position of the phosphate of heptulose-2-*P* (Johnson et al., 1990). The X-ray results suggest that by binding at the catalytic site the NJT creates a phosphate-recognition site and that there is a synergy between the two ligands. The phosphorus-phosphorus distance between the phosphate and 5′-phosphate of PLP is 4.7 Å and there is a direct hydrogen bond between the two phosphate oxygens. The binding of NJT and phosphate in the T state GP*b*, is accompanied by certain local conformational changes in the vicinity of the catalytic site. The greatest changes include shifts of the main-chain and side-chain atoms of Leu 136 by approximately 0.5 Å away from the catalytic site to accommodate the additional nitrogen ring and

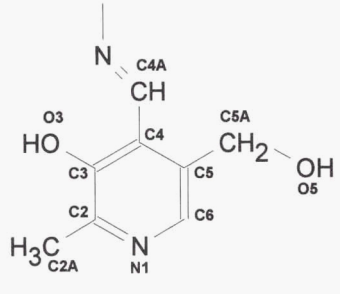

Scheme II. Bound PL, showing the numbering system used.

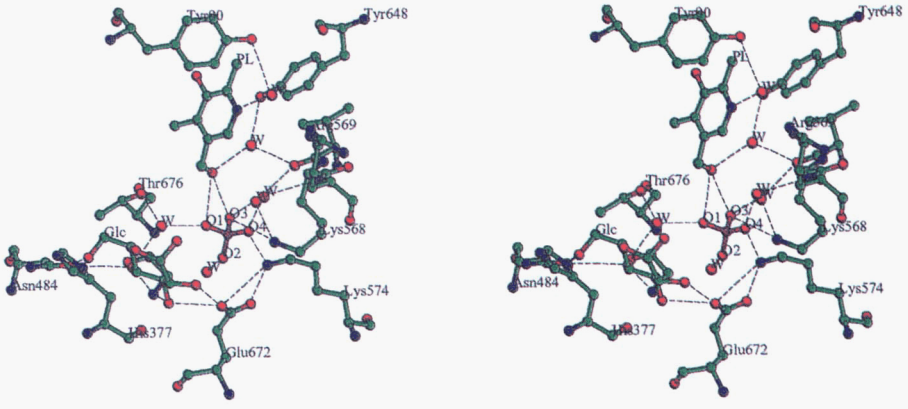

Fig. 4. The contacts between phosphate, Glc, and catalytic site residues of T-state PL-GP*b*-phosphate-Glc-IMP complex. The view is similar to those shown in Figures 2 and 3.

a shift of the guanidinium group of Arg 569 by over 7 Å from its native position. When Arg 569 undergoes a large conformational change, the 280s loop becomes disordered with the acidic residue Asp 283 moving out of the site, indicating that the catalytic site becomes more R-state-like.

Superposition of the structure of the PL-GP*b*-phosphate-Glc-IMP complex with the structure of the GP*b*-NJT-phosphate complex was performed (with IMPOSE) to construct a rough model of the ternary complex of phosphate anion activated PL-GP*b*, substrate phosphate, and NJT (Fig. 5). The comparison showed that these structures are quite similar and superimpose quite well. After superimposition the RMS deviation (RMSD) was 0.38 and 0.37 Å for C^{α} and backbone atoms, respectively, for residues 14–839. These numbers reduce to 0.30 and 0.29 Å if the least well ordered parts of the structure are omitted (residues 252–260, 315–324, 835–839). The one significant difference between the two structures lies in the conformation of Arg 569, which, in the GP*b*-NJT-phosphate complex, occupies a position close to that occupied by Asp 283 in the PL-GP*b*-phosphate-Glc-IMP complex. It is also noteworthy that the distance between the phosphate anion in the

Table 3. *Hydrogen-bond interactions between PL and phosphate and residues of the catalytic site of T-state PL-GPb*

	Protein atoms		
Ligand atoms	1st[a]	2nd[a]	3rd[a]
PL			
N-1	Wat 3.896 (2.8)[b]	Tyr 90 OH (3.3)	
		Asn 133 O (3.2)	
		Wat 0.884 (3.0)	Lys 608 N (3.0)
O-5	Wat 2.895 (2.8)	Tyr 648 OH (2.7)	
		Val 567 O (2.7)	
	OP-3 (2.7)		
Phosphate			
OP-1	Wat 1.897 (2.6)	O-4 Glc (2.7)	
		Thr 676 N (3.2)	
		Thr 676 OG1 (2.7)	
OP-2	Wat 0.885 (2.7)	Gln 665 OE1 (2.9)	Lys 568 NZ (2.8)
		Wat 9.896 (3.0)	Asn 696 OD1(3.1)
			Ser 674 O (2.9)
OP-3	O-5 PL (2.7)		
	Lys 568 NZ (2.9)	Gln 665 OE1 (2.8)	
	Wat 1.895 (2.8)	Val 567 O (3.1)	
		Gln 665 NE2 (3.1)	Wat 3.882 (3.2)
		Lys 568 NZ (2.7)	
		Wat 3.882 (3.3)	Gln 665 NE2(3.2)
			Val 567 N (3.1)
			Glu 664 O (3.2)
OP-4	Lys 574 NZ (2.7)		
	Wat 0.879 (2.7)	Arg 569 N (2.9)	—

[a] 1st, 2nd, and 3rd represent the 1st, 2nd, and 3rd coordination protein atoms.
[b] Values in parentheses represent hydrogen bond distances in Å.

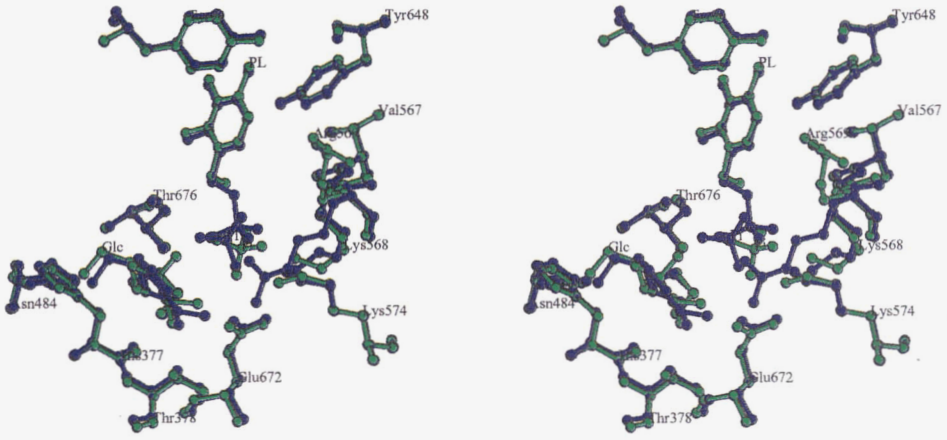

Fig. 5. Superposition of residues in T-state PL-GP*b*-phosphate-Glc-IMP and T-state PLP-GP*b*-phosphate-NJT complex in the vicinity of the catalytic site. Green, co-crystallized PL-GP*b*-phosphate-Glc-IMP complex; blue, PLP-GP*b*-phosphate-NJT complex (Mitchell et al., 1996).

PL-GP*b*-phosphate-Glc-IMP complex and the substrate phosphate in the GP*b*-NJT-phosphate complex is 4.6 Å.

Discussion

Previous ultracentrifugation and crystallization studies of GP reconstituted with modified cofactors have provided a structural test on the allosteric properties of these derivative enzymes. PL, DPL, PLPMe, or PLDP reconstituted GPs, which in solution exhibit properties of the R state and tetramerize in the presence of the nucleotide activator, fail to crystallize under conditions that favor T-state enzyme. Addition of the T-state inhibitor Glc to the IMP activated PL-GP*b*-anion tetrameric complex results in complete conversion to the dimeric form and induces crystallization (Oikonomakos et al., 1987; this study). It is interesting that Glc does not bind to the PL-GP*b* in the T state in the absence of anion, and vice versa. DPL-GP*b*, PLPMe-GP*b*, and PLDP-GP*b* cannot be crystallized in the T-state form, possibly because Glc cannot bind (or binds weakly) to these enzymes (Yan et al., 1979; Withers et al., 1982b; Leonidas et al., 1992b; Sprang et al., 1992; Oikonomakos et al., unpubl.). Thus, any substitutions of PLP that favor the formation of Glc binding site are expected to trigger the R- to T-state conformation change. The ultracentrifugation data reported previously (Withers et al., 1982b) and in this study show that in order for Glc to bind either to AMP- or IMP-activated PL-GP*b*, phosphite should be bound. Dissociation of tetramers to dimers is observed only in the presence of both ligands. Our kinetic, ultracentrifugation, and crystallographic results show that Glc, a poor inhibitor of the R-state PL-GP*b*, is an indispensable structural determinant of the dimeric T-state PL-GP*b*-phosphite enzyme for which it exhibits a higher affinity. Although the two ligands Glc and anion do not interact directly in the PL-GP*b*-phosphate-Glc-IMP complex, phosphate oxygen OP-1 interacts with O-4 hydroxyl of Glc via a water molecule (Table 3).

The crystal structures of the PL-GP*b*-anion-Glc-IMP complexes show that the activator anions bind strongly at the catalytic site in a similar but not identical position (shifts of approximately 1.2 Å) to that occupied by the 5′-phosphate group of PLP in the native enzyme. On the basis of kinetic and ^{19}F-NMR studies with PL-GP*b*, the O-5 group was identified as having structural and catalytic importance. Substitution of this group in PL-GP*b* by a -H in DPL-GP*b* affects both phosphite binding and enzymic activity. Thus, the dissociation constant of phosphite is approximately ten times higher, and V_{max} decreases from 15.4 (PL-GP*b*) to 2.8 units/mg in the DPL-GP*b* (Chang et al., 1987). These differences were attributed to the lack of a hydrogen bond between the O-5 of PL and phosphite in the latter derivative (Chang et al., 1983, 1987). The crystallographic results on the PL-GP*b*-anion-Glc-IMP complexes indicate that the closest distance between O-5 and activating phosphate oxygen OP-3 (Table 3) is 2.7 Å, which is sufficiently short to assume a hydrogen bond.

The catalytic mechanism of GP has been extensively investigated (Madsen & Withers, 1986; Johnson et al., 1989; Palm et al., 1990; Oikonomakos et al., 1992; Sprang et al., 1992) and we briefly review the evidence leading to the two main proposals (Scheme III). Both proposals depend on the correct positioning of the substrate phosphate with respect to the cofactor 5′-phosphate. Substantial evidence in favor of the acid-base mechanism (Scheme IIIA) comes from the direct experimental proof of protonation of glycosylic substrates, compounds of nonglycosidic structure with the anomeric C1 linked via an electron-rich bond (Klein et al., 1982, 1984, 1986). Thus it has been shown that an enzyme-derived proton attacks endocyclic or exocyclic double bond of D-glucal or heptenitol and the activated sugar moiety is subsequently transferred to an acceptor. The strongest evidence for the direct phosphate–phosphate interaction comes from time resolved studies on the conversion of heptenitol to heptulose 2-*P* and the crystallographic analysis of the T-state GP*b*-heptulose-2-*P* complex (Hajdu et al., 1987; Johnson et al., 1990; Duke et al., 1994). The close proximity of the product phosphate to the cofactor 5′-phosphate provides support for a mechanism in which phosphorolysis of heptenitol is catalyzed by general acid attack of the substrate phosphate, promoted by the cofactor 5′-phosphate. The recent X-ray work with NJT and phosphate (Mitchell et al., 1996) also show directly that the substrate phosphate binding site is in the correct position for the general acid attack. The proton is donated by the substrate phosphate in a concerted reaction in which it immediately gains a proton from the cofactor 5′-phosphate. Thus, the mechanism relies on the correct disposition of the two phosphate groups in order to promote catalysis. The electrophilic mechanism

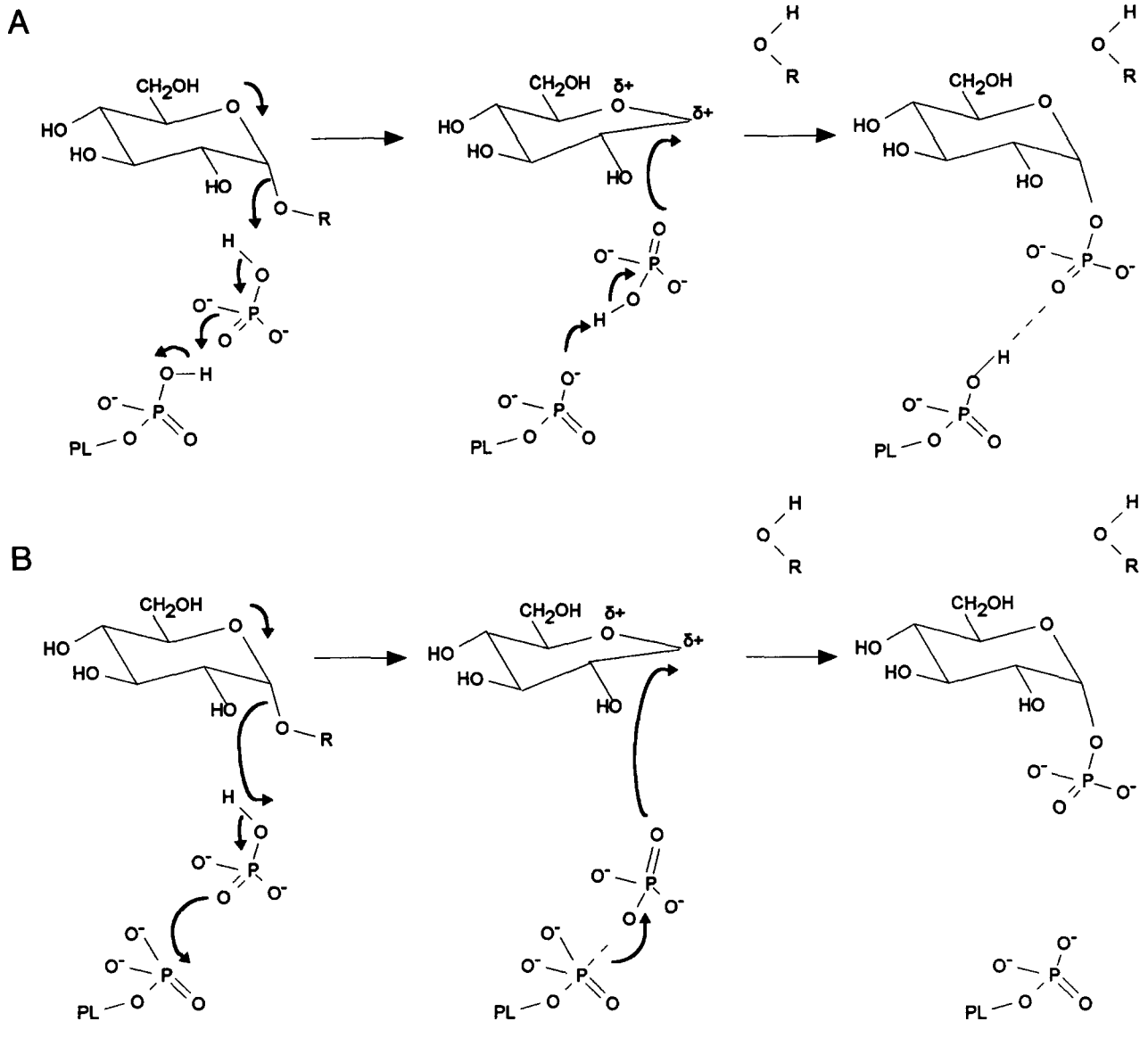

Scheme III. Proposals for the catalytic mechanism. **A**: The PLP acts as a general acid-base to promote attack by the substrate phosphate. **B**: The PLP acts as an electrophile to withdraw electrons and promote attack by the substrate phosphate.

(Scheme IIIB) is mainly supported from studies with PLDP-Glc reconstituted GP (Withers et al., 1981; Takagi et al., 1982). This enzyme derivative was shown to catalyze stereospecific glucosyl transfer from the bound coenzyme analogue to glycogen, suggesting a similar binding mode of the Glc-1-*P* in the native enzyme. However, the PLDP-Glc reconstituted GP*b* has a very low activity and catalyzes a rather unusual reaction that is not part of the normal reaction pathway. In the electrophilic mechanism, a closer association between the cofactor and substrate phosphates is required than has been observed in the crystallographic results to date. Such a close approach is mimicked by PLDP, but the structural studies on the R-state GP*b*-PLDP complexes (Leonidas et al., 1992b; Sprang et al., 1992) showed no evidence of additional strong interactions with the cofactor 5′-phosphate that have been invoked to provide stabilizing energy for the constrained activator dianion (Chang et al., 1983; Madsen & Withers, 1986; Sprang et al., 1992) as one might have expected on the basis of this mechanism.

A main argument against a role for the cofactor 5′-phosphate group as an acid in GP catalysis comes from the finding that fluorophosphate with a pK_a of 4.8 is as effective as phosphite (pK_a = 6.6) in activating PL-GP*b* (Parrish et al., 1977). The present results on the PL-GP*b*-anion complex structures have provided conclusive evidence for the location of the activator anion binding site. The positions of the phosphite, fluorophosphate, and phosphate at the catalytic site are indistinguishable and it seems likely that all the anion activated PL-GP*b* complexes share a common catalytic process. The activity with PL-GP*b* plus phosphite is 15% that of the PLP-GP*b* (Table 1) and the X-ray studies show that the noncovalently bound phosphite is 1.2 Å from the PLP phosphate position. This is sufficiently large to be taken into account for a mechanism that relies on the correct disposition of the two phosphate groups in order to promote catalysis. The noncovalent anions do not bind in PL-GP*b* to the same position to which these anions bind when linked covalently to the O-5 of PL and this may explain

why they are less active. Superposition of the structures of the PL-GP*b*-phosphate-Glc-IMP and GP*b*-NJT-phosphate complexes (Fig. 5) suggests that if the anion were to be incorporated in the GP*b*-NJT-phosphate complex structure, it would located approximately 4.6 Å from the substrate phosphate. Though this result could be consistent with the electrophilic mechanism, there is no experimental evidence. The close approach of two phosphate groups in other enzymes such as the kinases is usually stabilized by magnesium ions (Johnson et al., 1996). GP does not require magnesium ions although there is a bridging water between the two phosphates in the GP*b*-NJT-phosphate complex structure (Mitchell et al., 1996). Klein et al. (1984) have suggested that a slightly different structure of the PL-GP*b*-anion enzyme compared with the native holoenzyme might bring in a proton donor group of the enzyme that normally is not in the reaction path. The similarity of the pH profiles of PL-GP*b* activated with either phosphite or fluorophosphate (Withers et al., 1982c) was also taken to support this assumption. We suggest that the activator anion in PL-GP*b* may play an important role in maintaining the catalytic site structure for effective catalysis to occur. The assignment of an amino acid side chain as proton donor in PL-GP*b* catalytic mechanism, however, is not possible, because at present, we are only limited to static observation of the unliganded T-state PL-GP*b*-anion complexes. In the absence of data concerning the ternary complex of the enzyme with its natural substrates, a detailed description, in molecular terms, of the mechanism cannot be given. The bound anion position observed here might represent a fortuitous binding site recognized by the T-state enzyme. Binding of one of the pairs or both of the natural substrates Glc-1-*P* (or phosphate) and oligosaccharide may be accompanied by conformational changes, resulting in relocalization of catalytic groups that are not properly positioned in the present structures. Whether PL-GP*b*-anion enzyme follows a different mechanism from that of the native PLP-GP*b*, by using an amino acid side chain as an acid-base group, requires the determination of the crystal structure of the ternary complex. Attempts to crystallize both binary and ternary complexes of PL-GP*b* are in progress.

Materials and methods

PL, AMP, Glc-1-*P* (dipotassium salt), glycogen, and other chemicals were obtained from Sigma Chemical Co. (St. Louis, MO). Oyster glycogen (purchased from Sigma Chemical Co.) was freed of AMP by the method of Helmreich & Cori (1964).

Preparation of phosphorylase, apophosphorylase, and pyridoxal phosphorylase

GP*b* was isolated from rabbit skeletal muscle according to Fischer & Krebs (1962) using 2-mercaptoethanol instead of L-cysteine and recrystallized at least four times. Bound nucleotides were removed from the enzyme as previously described (Melpidou & Oikonomakos, 1983). Protein concentration was determined from absorbance measurements at 280 nm using an absorbance index $A^{1\%}_{1\,cm} = 13.2$ (Kastenschmidt et al., 1968). Apo-GP*b* was prepared by the method of Withers et al. (1982a). Assays of this apoenzyme showed no activity and could be reconstituted with an eight-fold excess of PLP to normal activity. The procedure for the reconstitution of apo-GP*b* with a 50-fold excess of PL has been described previously (Oikonomakos et al., 1987).

Determination of phosphorylase activity

GP*b* and PL-GP*b* activities were measured at pH 6.8 and 30 °C in the direction of glycogen synthesis by the release of orthophosphate from Glc-1-*P*. The enzymes (GP*b*: 5–10 μg/ml or PL-GP*b*: 25–50 μg/ml) were assayed in 20 mM β-glycerophosphate (pH 6.8), 15 mM 2-mercaptoethanol, 1 mM EDTA, 1% glycogen, 1 mM AMP, and a range of concentrations of Glc-1-*P* and phosphite (for PL-GP*b* activation), as indicated in the footnote of Table 1. The enzymes were preincubated with glycogen for 15 minutes at 30 °C before the reaction was started by adding Glc-1-*P*. Samples were withdrawn at 1-minute intervals over the period from 1–5 minutes and transferred into 0.2% sodium dodecyl sulphate to stop the reaction. Inorganic phosphate released in the GP reaction was determined according to Fiske and Subbarow (1925). Initial rates of reaction, v, were calculated from the pseudo-first-order reaction constants (Leonidas et al., 1992a) by using a non-linear-regression data analysis program (GraFit) and assuming the standard error, σ^2, is the same for each data point ("simple weighting") (Leatherbarrow, 1992). The program calculated the reaction rates and the standard errors of these values. Kinetic data transformed in the form of Hill plots were treated by linear-regression analysis by providing an explicit value for the standard deviation of each rate ("explicit weighting"). K_i values at each concentration of inhibitor were then determined by plotting K_m(app) versus inhibitor concentration using the same type of analysis.

Ultracentrifugation

Ultracentrifugation experiments were performed on a MSE Centriscan 75 analytical ultracentrifuge with 10 mg/ml PL-GP*b* in 7 mM β-glycerophosphate, 7 mM 2-mercaptoethanol buffer, pH 6.8, at a rotor speed of 50,000 rpm and a temperature of 20 °C. Sedimentation coefficients calculated from direct measurements of the scanner traces were corrected for the viscosity and density of the buffer to water at 20 ± 1 °C (Oikonomakos et al., 1985; Leonidas et al., 1992a). Traces were taken 20–50 minutes after attainment of speed of 50,000 rpm. The percentage of the components with different sedimentation coefficients was estimated by measuring the area under the sedimentation peaks and above the base line by cutting out the required area and weighing it (MSE Technical Publication No. 73, Supplement). Error in the estimation of areas of poorly resolved components (or minor peaks) was less than 20%.

X-ray crystallography

T-state PL-GP*b* was co-crystallized with 8–10 mM phosphite, 8–10 mM phosphate, or 8–10 mM fluorophosphate in a medium consisting of 15–25 mg/ml enzyme, 2 mM IMP, 2 mM spermine, 50 mM Glc, 10 mM Bes, 0.1 mM EDTA, and 0.02% sodium azide, pH 6.7 (16 °C). Co-crystals of T-state PL-GP*b*-anion-Glc-IMP complexes were grown within a few days in space group $P4_32_12$, with native-like unit cell dimensions (Acharya et al., 1991). Just before data collection, the crystals were transferred to a fresh buffer solution containing the same constituents as their mother liquor, with the exception of the protein. Three-dimensional data to 2.4 Å resolution were collected on an Arndt-Wonacott oscillation camera at the SERC Synchrotron Radiation Source at Daresbury, UK (Station 7.2) (Helliwell et al., 1982). The wavelength was 1.488 Å, and the synchrotron was operated at 2.0 GeV with current ranging from 250–150 mA. Two crystals were used for each enzyme complex and aligned with c^* coincident with the crystal rotation axis. Data

were recorded on contiguous packs with spindle oscillation range ($\Delta\phi$) of 1.5 degrees per film pack and a speed varied from 20–75 s/deg. Collimator aperture size was 0.6 mm, and a total of 32 packs (three films per pack), for each experiment, corresponding to a rotation range of $\phi = 48$ degrees, were recorded. The films were scanned with a 50-μm raster with an Optronics Microdensitometer. Crystal orientations were determined using STILLS (A.G.W. Leslie et al., unpubl.) and REFIXNEW (Kabsch, 1988). Intensities were integrated with a modified version (D.I. Stuart et al., unpubl.) of MOSCO (Nybourg & Wonacott, 1977). Standard corrections and subsequent scaling of the films were carried out with ABSCALE, AGROVATA, ROTAVATA, and ANISOSC (see Barford et al., 1991; Leonidas et al., 1992b) to produce scaled sets of structure factors, which were then used to generate difference Fourier electron density maps (with respect to the native protein) (Acharya et al., 1991) using the CCP4 suite of programs for protein crystallography (Collaborative Computation Project, No. 4, 1994). Partial charges on the anions were estimated using AM1 calculations with MOPAC. Partial charges and energy parameters for Glc and IMP were those provided in X-PLOR (Brunger, 1992) for the glucopyranose ring and nucleic acid, respectively. The three structures were refined with similar protocols by using X-PLOR energy and crystallographic least-squares minimization (Brunger, 1992). The starting protein structure was the refined structure of the T-state GP*b*-1-GlcNac-IMP complex (Oikonomakos et al., 1995). Water molecules in the PL-GP*b*-anion-Glc-IMP complexes were examined, and those displaced by the ligands were removed. The initial structure *R* factors were 22.8%, 23.4%, and 21.5%, which fell to 19.2%, 18.5%, and 18.5% for the phosphite, phosphate, and fluorophosphate complexes, respectively, after 130 cycles of positional refinement and 60 cycles of *B* factor refinement. Final SIGMAA-weighted $2F_o - F_c$ maps (Read, 1986) were examined for satisfactory fit of atoms to the electron density. Estimates of the precision of coordinates taken from previous studies (Martin et al., 1990) indicate errors of the order of 0.2 Å. The average *B*-factors for main-chain atoms were 22, 21, and 20 Å^2 for phosphite, phosphate, and fluorophosphate complexes, respectively. Examination of *B*-factor plots and the final electron density maps showed that residues 251–260, 314–325, and 831–839 were not well ordered. A correction for the bulk solvent was not applied and the low resolution cut off was 8 Å. The omission of low resolution terms may account for the low electron density for parts of the molecule noted as being poorly ordered. However, these same regions are also poorly ordered in the structure of the native enzyme where low resolution terms and a bulk solvent correction were included in the refinement (Acharya et al., 1991). The statistics for data collection, processing, and refinement are shown in Table 2.

The structures were analyzed with FRODO (Jones, 1985) and O (Jones et al., 1991) on an ESV-10 graphics terminal. Hydrogen-bonds were assigned if the distance between the electronegative atoms was less than 3.3 Å and if both angles between these atoms and the preceding atoms were greater than 90 degrees. Van der Waals interactions were assigned for non-hydrogen atoms separated by less than 4 degrees. Protein structural changes were calculated, by superimposition of different muscle GP coordinate sets, with the program IMPOSE (Esnouf, 1992). The program takes two files of coordinates for a molecule and superimposes the second on the first using ranges of coordinates in both structures by using the FORTRAN subroutine MATFIT (S.J. Remington, unpubl.). This subroutine calculates the RMSD between two sets of atomic coordinates and the rotation matrix and translation vector that best superposes the position vector of two sets of atoms. Coordinate sets for comparison were: T-state GP*b* (Acharya et al., 1991) (PDB code 1GPB), T-state GP*b*-Glc complex (Martin et al., 1990) (PDB code 2GPB), T-state GP*b*-1-GlcNAc-IMP complex (Oikonomakos et al., 1995) (PDB code 1PRJ), and T-state GP*b*-phosphate-NJT complex (Mitchell et al., 1996) (PDB code 1NOJ).

Coordinates for T-state PL-GP*b*-fluorophosphate-Glc-IMP, PL-GP*b*-phosphate-Glc-IMP, and PL-GP*b*-phosphite-Glc-IMP complexes have been deposited with the Protein Data Bank, Brookhaven National Laboratory, Upton, NY 11973 (PDB ID Codes 1SKC, 1SKD, and 1SKE, respectively).

Acknowledgments

Support by the Daresbury Laboratory, under the minor grants scheme and the EU Large Facilities Programme (NGO), and by a research fellowship, ERBCHBI CT94 1232, under the Human Capital and Mobility Programme (NGO) is gratefully acknowledged. LNJ is a member of the Oxford Centre for Molecular Sciences. We are grateful to Ms. Evangelia Chryssina for help in the kinetic experiments. We also thank Dr. A.C. Papageorgiou and Dr. D.D. Leonidas for their initial contributions to the project. Figures 2–5 were produced using the program XOBJECTS (M.E.M. Noble, unpublished).

References

Acharya KR, Stuart DI, Varvill KM, Johnson LN. 1991. *Glycogen phosphorylase: Description of the protein structure*. World Scientific Publishers, Singapore and London.

Barford D, Hu SH, Johnson LN. 1991. Structural mechanism for glycogen phosphorylase control by phosphorylation and AMP. *J Mol Biol 218*:233–260.

Barford D, Johnson LN. 1989. The allosteric transition of glycogen phosphorylase. *Nature 340*:609–616.

Brunger AT. 1992. *X-PLOR Version 3.1. A system for X-ray crystallography and NMR*. New Haven and London: Yale University Press.

Chang YC, McCalmont T, Graves DJ. 1983. Functions of the 5′-phosphoryl group of pyridoxal 5′-phosphate in phosphorylase: A study using pyridoxal-reconstituted enzyme as a model system. *Biochemistry 22*:4987–4993.

Chang YC, Scott RD, Graves DJ. 1987. Function of pyridoxal 5′-phosphate in glycogen phosphorylase: A model study using 6-fluoro-5′-pyridoxal- and 5′-deoxy-pyridoxal-reconstituted enzymes. *Biochemistry 26*:360–367.

Collaborative Computational Project, Number 4. 1994. The CCP4 Suite: Programs for protein crystallography. *Acta Crystallogr D 50*:760–763.

Copley RR, Barton GJ. 1994. A structural analysis of phosphate and sulphate binding sites in proteins. Estimation of propensities for binding and conservation of phosphate binding sites. *J Mol Biol 242*:321–329.

Duke EMH, Wakatsuki S, Hadfield A, Johnson LN. 1994. Laue and monochromatic diffraction studies on catalysis in phosphorylase *b* crystals. *Protein Sci 3*:1178–1196.

Ermert P, Vasella A, Weber M, Rupitz K, Withers SG. 1993. Configurationally selective transition-state analog inhibitors of glycosidases. A study with nojiritetrazoles, a new class of glycosidase inhibitors. *Carbohydr Res 250*:113–128.

Esnouf RM. 1992. *Protein structure from simulated NMR databases*. Oxford, UK: University of Oxford.

Feldman K, Hull WE. 1977. ^{31}P nuclear magnetic resonance studies of glycogen phosphorylase from rabbit muscle: Ionisation states of pyridoxal 5-phosphate. *Proc Natl Acad Sci USA 74*:856–860.

Fischer EH, Kent AB, Snyder ER, Krebs EG. 1958. Reaction of sodium borohydride with rabbit muscle phosphorylase. *J Am Chem Soc 80*:2906–2907.

Fischer EH, Krebs EG. 1962. Muscle phosphorylase *b*. *Methods Enzymol 5*:369–373.

Fiske CH, Subbarow Y. 1925. The colorimetric determination of phosphorous. *J Biol Chem 66*:375–400.

Graves DJ, Wang JH. 1972. α-Glucan phosphorylases—Chemical and physical basis of catalysis and control. In: Boyer PD, ed., *The Enzymes*, 3rd ed. Vol. 7. New York: Academic Press. pp 435–482.

Hajdu J, Acharya KR, Stuart DI, McLaughlin PJ, Barford D, Oikonomakos NG, Klein H, Johnson LN. 1987. Catalysis in the crystal: Synchrotron radiation studies with glycogen phosphorylase *b*. *EMBO J 6*:539–546.

Helliwell JR, Greenhough TJ, Carr PD, Rule SA, Moore PR, Thompson AW, Worgan JS. 1982. A central data collection facility for protein crystallography, small angle diffraction and scattering with the Daresbury Laboratory synchrotron radiation source. *J Phys E15*:1363–1372.

Helmreich EJM, Cori CF. 1964. The role of adenylic acid in the activity of phosphorylase. *Proc Natl Acad Sci USA 51*:131–138.

Johnson LN. 1992. Glycogen phosphorylase: Control by phosphorylation and allosteric effectors. *FASEB J 6*:2274–2282.

Johnson LN, Acharya KR, Jordan MD, McLaughlin PJ. 1990. Refined crystal structure of the phosphorylase heptulose-2-phosphate-oligosaccharide-AMP complex. *J Mol Biol 211*:645–661.

Johnson LN, Hajdu J, Acharya KR, Stuart DI, McLaughlin PJ, Oikonomakos NG, Barford D. 1989. Glycogen phosphorylase *b*. In: Herve G, ed., *Allosteric enzymes*. Boca Raton, FL: CRC Press. pp 81–127.

Johnson LN, Noble MEM, Owen DJ. 1996. Active and inactive protein kinases: Structural basis for regulation. *Cell 85*:149–158.

Jones TA. 1985. Interactive computer graphics: FRODO. *Methods Enzymol 115*:157–171.

Jones TA, Zou JY, Cowan SW, Kjeldgaard M. 1991. Improved methods for the building of protein models in electron density maps and the location of errors in these models. *Acta Crystallogr A47*:110–119.

Kabsch WJ. 1988. Evaluation of single crystal X-ray diffraction data for a position-sensitive detector. *J Appl Crystallogr 21*:916–924.

Kastenschmidt LL, Kastenschmidt J, Helmreich EJM. 1968. Subunit interactions and their relationship to the allosteric properties of rabbit skeletal muscle phosphorylase *b*. *Biochemistry 7*:3590–3608.

Klein HW, Im MJ, Palm D. 1986. Mechanism of the phosphorylase reaction. Utilization of D-gluco-hept-1-enitol in the absence of primer. *Eur J Biochem 157*:107–114.

Klein HW, Im MJ, Palm D, Helmreich EJM. 1984. Does pyridoxal 5′-phosphate function in glycogen phosphorylase as an electrophilic or a general acid catalyst? *Biochemistry 23*:5853–5861.

Klein HW, Palm D, Helmreich EJM. 1982. General acid-base catalysis of α-glucan phosphorylases: Stereospecific glucosyl transfer from D-glucal is a pyridoxal 5′-phosphate and orthophosphate (arsenate) dependent reaction. *Biochemistry 21*:6675–6684.

Leatherbarrow RJ. 1992. *GraFit Version 3.0*. Erithakus Software, Staines, UK.

Leonidas DD, Oikonomakos NG, Papageorgiou AC. 1992a. Kinetic properties of tetrameric glycogen phosphorylase *b* in solution and in the crystalline state. *Protein Sci 1*:1123–1132.

Leonidas DD, Oikonomakos NG, Papageorgiou AC, Acharya KR, Barford D, Johnson LN. 1992b. Control of phosphorylase *b* by a modified cofactor: Crystallographic studies on R-state glycogen phosphorylase reconstituted with pyridoxal 5′-diphosphate. *Protein Sci 1*:1112–1122.

Madsen NB. 1986. Glycogen phosphorylase: Control by phosphorylation. In: Boyer PD, Krebs EG, eds., *The enzymes*, 3rd ed. Vol. 17. New York: Academic Press, pp 366–394.

Madsen NB, Withers SG. 1986. Glycogen phosphorylase. In: Dolphin D, Poulson R, Avramovic O, eds., *Coenzymes and cofactors, Vol. I. Vitamin B_6 pyridoxal phosphate*. New York: John Wiley. pp 355–389.

Martin JL, Johnson LN, Withers SG. 1990. Comparison of the binding of glucose and glucose-1-phosphate derivatives to T state glycogen phosphorylase *b*. *Biochemistry 29*:10745–10757.

Martin JL, Veluraja K, Johnson LN, Fleet GWJ, Ramsden NG, Bruce I, Orchard MG, Oikonomakos NG, Papageorgiou AC, Leonidas DD, Tsitoura HS. 1991. Glucose analogue inhibitors of glycogen phosphorylase: The design of potential drugs for diabetes. *Biochemistry 30*:10101–10116.

McLaughlin PJ, Stuart DI, Klein HW, Oikonomakos NG, Johnson LN. 1984. Substrate-cofactor interactions for glycogen phosphorylase *b*: A binding study in the crystal with heptenitol and heptulose-2-phosphate. *Biochemistry 23*:5862–5873.

Melpidou AE, Oikonomakos NG. 1983. Effect of glucose-6-P on the catalytic and structural properties of glycogen phosphorylase. *FEBS Lett 154*:105–110.

Mitchell EP, Withers SG, Ernert P, Vasella AT, Garman EF, Oikonomakos NG, Johnson LN. 1996. Ternary complex structures of glycogen phosphorylase with the transition state analogue nojirimycin tetrazole and phosphate in the T and R states. *Biochemistry 35*:7341–7355.

Monod J, Changeux JP, Jacob F. 1965. On the nature of allosteric transitions: A plausible model. *J Mol Biol 12*:88–118.

Newgard CB, Hwang PK, Fletterick RJ. 1989. The family of glycogen phosphorylases: Structure and function. *Crit Rev Biochem Mol Biol 24*:69–99.

Nybourg J, Wonacott AJ. 1977. Computer programmes. In: Arndt UW, Wonacott AJ, eds., *The rotation method in crystallography*. Amsterdam: North-Holland. pp 139–152.

Oikonomakos NG, Acharya KR, Johnson LN. 1992. Rabbit muscle glycogen phosphorylase *b*: Structural basis of activation and catalysis. In: Harding JJ, Crabbe MJC, eds., *Post-translational modification of proteins*. Boca Raton, FL: CRC Press. pp 81–151.

Oikonomakos NG, Acharya KR, Melpidou AE, Stuart DI, Johnson LN. 1989. The binding of glycerol 2-*P* to glycogen phosphorylase *b* in the crystal. *Arch Biochem Biophys 269*:62–68.

Oikonomakos NG, Johnson LN, Acharya KR, Stuart DI, Barford D, Hajdu J, Varvill KM, Melpidou AE, Papageorgiou AC, Graves DJ, Palm D. 1987. Pyridoxal phosphate site in glycogen phosphorylase: Structure in native enzyme and in three derivatives with modified cofactors. *Biochemistry 26*:8381–8389.

Oikonomakos NG, Kontou M, Zographos SE, Watson KA, Johnson LN, Bichard CJF, Fleet GWJ, Acharya KR. 1995. N-acetyl-beta-D-glucopyranosylamine: A potent T-state inhibitor of glycogen phosphorylase. A comparison with alpha-D-glucose. *Protein Sci 4*:2469–2477.

Oikonomakos NG, Melpidou AE, Johnson LN. 1985. Crystallization of pig skeletal phosphorylase *b*. Purification, physical and catalytic characterization. *Biochim Biophys Acta 832*:248–256.

Palm D, Klein HW, Schinzel R, Buehner M, Helmreich EJM. 1990. The role of pyridoxal 5′-phosphate in glycogen phosphorylase catalysis. *Biochemistry 29*:1099–1107.

Parrish RF, Uhing RJ, Graves DJ. 1977. Effect of phosphate analogues on the activity of pyridoxal reconstituted glycogen phosphorylase. *Biochemistry 16*:4824–4831.

Rao ST, Sundaralingam M. 1969. Stereochemistry of nucleic acids and their constituents. V. The crystal and molecular structure of a hydrated monosodium inosine 5′-phosphate. A commonly occurring unusual nucleotide in the anticodons of tRNA. *J Amer Chem Soc 91*:1210–1217.

Read RJ. 1986. Improved Fourier coefficients for maps using phases from partial structures with errors. *Acta Crystallogr A 42*:140–149.

Segel IH. 1975. *Enzyme kinetics*. New York: Wiley-Interscience. pp 273–345.

Spiram M, Liaw YC, Go YC, Wang AHJ. 1991. Comparison of two hydrated forms of sodium inosine-5′-monophosphate. *Acta Crystallogr C47*:507–510.

Sprang SR, Acharya KR, Goldsmith EJ, Stuart DI, Varvill KM, Fletterick RJ, Madsen NB, Johnson LN. 1988. Structural changes in glycogen phosphorylase induced by phosphorylation. *Nature 336*:215–221.

Sprang SR, Goldsmith EJ, Fletterick RJ, Withers SG, Madsen NB. 1982. Catalytic site of glycogen phosphorylase: Structure of the T state and specificity for α-D-glucose. *Biochemistry 21*:5364–5371.

Sprang SR, Madsen NB, Withers SG. 1992. Multiple phosphate positions in the catalytic site of glycogen phosphorylase: Structure of the pyridoxal-5′-pyrophosphate coenzyme-substrate analog. *Protein Sci 1*:1100–1111.

Sprang SR, Withers SG, Goldsmith EJ, Fletterick RJ, Madsen NB. 1991. Structural basis for activation of glycogen phosphorylase *b* by adenosine monophosphate. *Science 254*:1367–1371.

Takagi M, Fukui T, Shimomura S. 1982. Catalytic mechanism of glycogen phosphorylase: Pyridoxal(5′)diphospho(1)-α-D-glucose as a transition-state analogue. *Proc Natl Acad Sci USA 79*:3716–3719.

Withers SG, Madsen NB, Sprang SR, Fletterick RJ. 1982a. Catalytic site of glycogen phosphorylase: Structural changes during activation and mechanistic implications. *Biochemistry 21*:5372–5382.

Withers SG, Madsen NB, Sykes BD. 1982b. Covalently activated glycogen phosphorylase: A phosphorus-31 nuclear magnetic resonance and ultracentrifugation analysis. *Biochemistry 21*:6716–6722.

Withers SG, Madsen NB, Sykes BD, Takagi M, Shimomura S, Fukui T. 1981. Evidence for the direct phosphate-phosphate interaction between pyridoxal phosphate and substrate in the glycogen phosphorylase catalytic mechanism. *J Biol Chem 256*:10759–10762.

Withers SG, Shechosky S, Madsen NB. 1982c. Pyridoxal phosphate is not the acid catalyst in the glycogen phosphorylase catalytic mechanism. *Biochem Biophys Res Commun 108*:322–328.

Yan SCB, Uhing RJ, Parrish RF, Metzler DE, Graves DJ. 1979. A role for pyridoxal phosphate in the control of dephosphorylation of phosphorylase *a*. *J Biol Chem 254*:8263–8269.